

Miniature lamellar grating interferometer based on silicon technology

Omar Manzardo, Roland Michaely, Felix Schädelin, Wilfried Noell, Thomas Overstolz, Nico De Rooij, and Hans Peter Herzig

Institute of Microtechnology, University of Neuchâtel, Breguet 2, 2000 Neuchâtel, Switzerland

Received January 23, 2004

We present a lamellar grating interferometer realized with microelectromechanical system technology. It is used as a time-scanning Fourier-transform spectrometer. The motion is carried out by an electrostatic comb drive actuator fabricated by silicon micromachining, particularly by silicon-on-insulator technology. For the first time to our knowledge, we measure the spectrum of an extended white-light source with a resolution of 1.6 nm at a wavelength of 400 nm and of 5.5 nm at 800 nm. The wavelength accuracy is better than 0.5 nm, and the inspected wavelength range extends from 380 to 1100 nm. The optical path difference maximum is 145 μm . The dimensions of the device are 5 mm \times 5 mm. © 2004 Optical Society of America

OCIS codes: 120.6200, 230.3990, 300.6300.

Spectrometry is widely used in industry and research laboratories. There are many different methods that are used in a variety of fields. In particular, Fourier-transform spectroscopy is a powerful technique for investigating weak sources with high resolution. At present, an extended range of Fourier spectrometers is commercially available. However, high resolution involves an elevated degree of mechanism precision and therefore large size and high cost. Recently, lower-resolution miniature spectrometers have become attractive because of new applications, expanding opportunities in a remarkable variety of disciplines and industries.¹ Miniaturization could make instruments and sensors easier to handle, faster, and cheaper. Such spectrometers have various applications, including color measurement, quality and process control, gas detection, and chemical analysis. Compact spectrometers are convenient in diverse fields, such as environmental monitoring, the food and beverage industry, imagery, telecommunication, life science, and medical diagnostics. Other specific aspects, such as dimensions and fabrication costs, play an important role in motivating the realization of small, portable sensor solutions. Most compact spectrometers use the dispersive effect of a grating. Few miniature instruments that exploit the advantages of Fourier spectroscopy have been developed² because of the high level of accuracy needed for their fabrication. Thanks to microelectromechanical system (MEMS) technology, by use of silicon micromachining, Fourier spectrometers can enter a new era.

A previous Letter³ presented a Fourier spectrometer based on silicon-on-insulator technology. The device was a Michelson interferometer with a scanning mirror. In this particular configuration the constraint is the necessity of incorporating a beam splitter. In fact, the integration of dedicated micro-optical elements into micromechanical systems becomes an issue of fabrication and handling. In addition, among different spectroscopic techniques exploiting MEMS technology,^{4,5} broadband measurement with a reasonable resolution is an issue. In this Letter we report on a MEMS-based Fourier spectrometer based on a lamellar grating interferometer. This concept

provides the advantage that it avoids the integration of the beam splitter. The device is capable of recording white-light spectra with a resolution comparable with that of a commercially available miniature grating spectrometer. The fabrication technology and the actuation concept are similar to the Michelson interferometer presented in Ref. 3.

A lamellar grating interferometer is a binary grating with a variable depth that operates in the zeroth order of the diffraction pattern. This type of apparatus was invented by Strong and Vanasse⁶ in 1960. A lamellar grating interferometer is used as a Fourier spectrometer, but, in contrast with a Michelson interferometer, which splits wave amplitudes at the beam splitter, a lamellar grating interferometer divides the wave front. At the grating the wave front is separated such that one half of the beam is reflected by the front facets (fixed mirrors) and one half by the back facets (mobile mirrors). Distance d between the two series of mirrors determines optical path difference (OPD) δ between the two parts of the wave (see Fig. 1). In general, this type of spectrometer is used for wavelengths larger than 100 μm ; below that level the tolerances

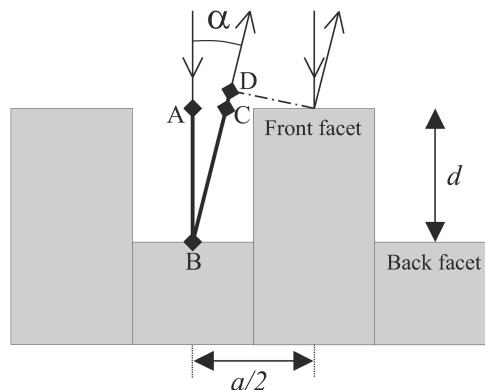


Fig. 1. Schematic of the lamellar grating interferometer. An incident wave front is divided by the front and back facets of a binary grating. The OPD δ between the beams reflected by the front and back facets is represented by the bold line and is given by Eq. (2). The OPD δ as a function of diffraction angle α and depth d of the grating is the sum of the distances AB, BC, and CD.

are too tight for most machine shops. Silicon micro-machining is the ideal technology to overcome these limitations for shorter wavelengths.

Intensity I of the diffraction pattern is given by⁶

$$I \propto \underbrace{\left(\frac{\sin K}{K}\right)^2}_{I_1} \underbrace{\left(\frac{\sin 2nK}{\sin 2K}\right)^2}_{I_2} \underbrace{\cos^2\left(\frac{\varphi}{2}\right)}_{I_3}, \quad (1)$$

where $K = (\pi a/2\lambda)\sin \alpha$, n is the number of illuminated periods, a is the grating period, and α is the diffraction angle. Phase shift $\varphi = (2\pi/\lambda)\delta$ is given by OPD δ , which is the sum of distances AB, BC, and CD in Fig. 1:

$$\delta = d\left(1 + \cos \alpha + \frac{a}{2d} \sin \alpha\right). \quad (2)$$

Intensity I of the diffraction pattern given by relation (1) has three contributions: I_1 is the sinc² function resulting from the rectangular shape of the grating period, I_2 is the comb function due to the periodicity of the grating (number of periods n and grating period a), and I_3 determines the phase shift due to grating depth d . These contributions are illustrated in Fig. 2 for a phase shift corresponding to $\varphi = M2\pi$ and $\varphi = \pi + M2\pi$ (M is an integer). When $\alpha = 0$ (zeroth order of the diffraction pattern), relation (1) reveals that intensity I modulates like a cosine as a function of the OPD $\delta = 2d$. The period of the modulation depends on wavelength λ . As a consequence, the basic equation of Fourier-transform spectroscopy,⁷

$$B(\sigma) = \int_{-\infty}^{\infty} I(\delta)\exp(-i2\pi\sigma\delta)d\delta, \quad (3)$$

where $\sigma = 1/\lambda$ is the wave number, applies to the lamellar grating interferometer. As in the case of the Michelson interferometer, the relation between I and δ is known as the interferogram, and power spectrum $B(\sigma)$ is the Fourier transform of the recorded intensity $I(\delta)$.

A scanning electron microscope photograph of the lamellar grating interferometer is shown in Fig. 3. The motion of the series of mirrors is carried out by an electrostatic comb drive actuator. The design concept and actuation principles are described in Ref. 1, and a diagram of the operation is shown in Ref. 3. The actuator is fabricated by deep reactive-ion etching of a silicon-on-insulator wafer. The fabrication process is described in Ref. 8. The height of the mirrors is 75 μm , the number of illuminated periods n of the grating is 12, the grating period is 90 μm , and the total dimensions of the device are 5 mm \times 5 mm. The quality of the surface of the mirrors is ensured by the fabrication technology. The surface roughness was measured to be 36 nm rms.

To demonstrate the ability of the spectrometer to inspect wide wavelength ranges with good resolution and accuracy, the spectrum of a low-pressure xenon arc lamp was measured. To carry out the measurement, the output light of a multimode fiber with a core diameter of 50 μm was collimated and the light

beam was focused with a cylindrical lens onto the grating. The focal length of the collimation lens was 10 mm, and the focal length of the cylindrical lens was 20 mm. The angle of incidence of the beam was zero, and the modulation of the zeroth order as a function of the OPD δ was measured with a photodiode detector. The recorded interferogram is shown in Fig. 4. The quality of the fringes and the symmetry of the interferogram demonstrate that there is no

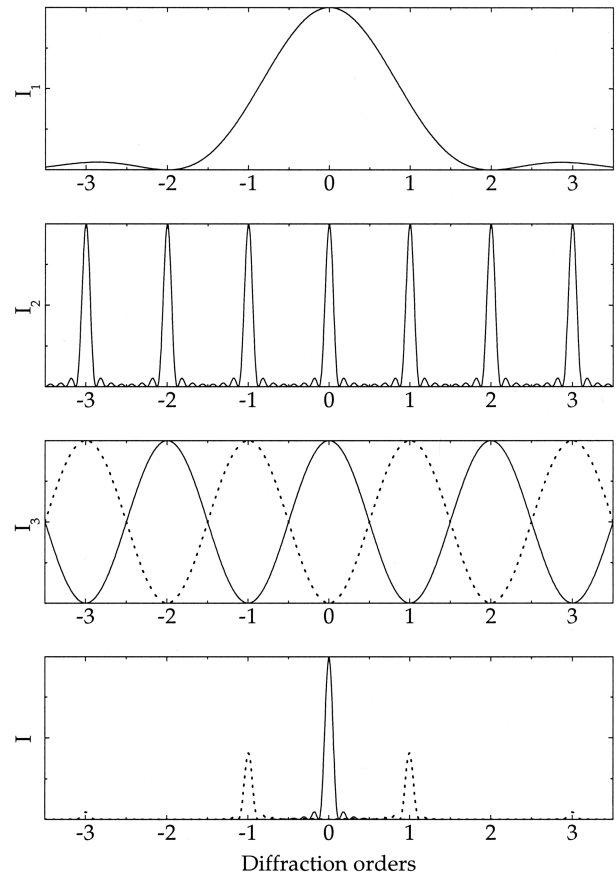


Fig. 2. Intensity I of the diffraction pattern of a lamellar grating [see relation (1)]. Intensity I is the multiplication of the three contributions, I_1 , I_2 , and I_3 , described in the text. The solid curve corresponds to a phase shift of $\varphi = M2\pi$, and the dotted curve corresponds to $\varphi = \pi + M2\pi$ (M is an integer).

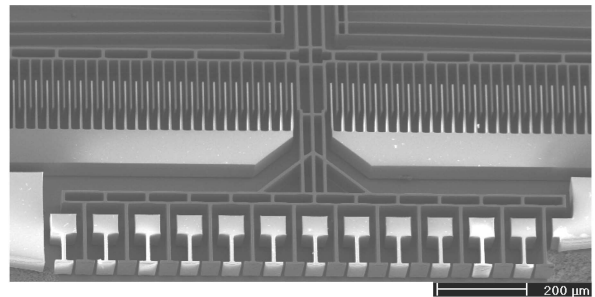


Fig. 3. Lamellar grating interferometer. One can distinguish the fixed (light) and mobile (dark) mirrors. The mobile mirrors are actuated by an electrostatic comb drive actuator. The motion is linear. The fabrication technology and the actuation principles are described in Refs. 1, 3, and 8.

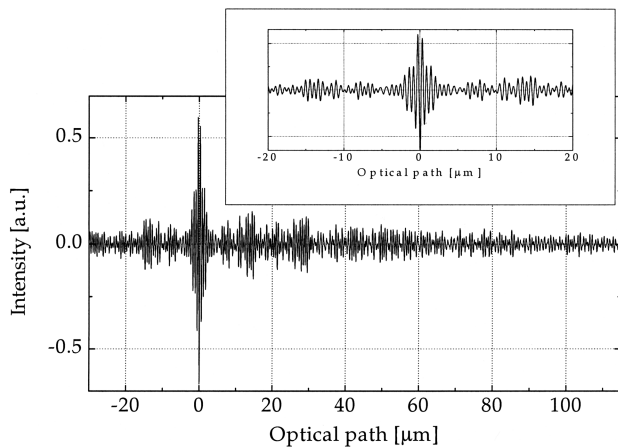


Fig. 4. Recorded interferogram of a low-pressure xenon arc lamp, with an expansion showing the OPD zero.

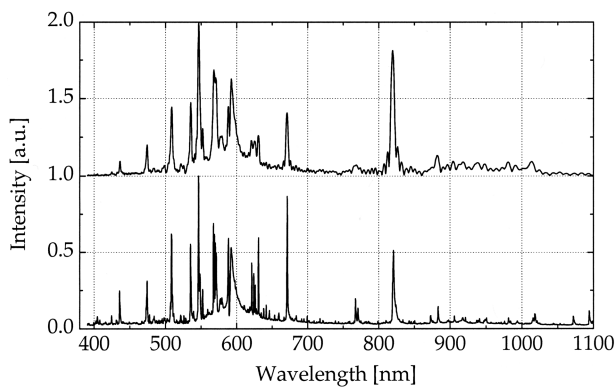


Fig. 5. Top, Power spectrum retrieved from the interferogram shown in Fig. 4. Bottom, Spectrum of the same lamp measured with a monochromator with a spectral resolution of 0.5 nm.

dispersive effect in the interferometer that could arise from the partially collimated beam. The center of the interferogram corresponds to the OPD zero. The OPD maximum achieved in this experiment was $145 \mu\text{m}$, which leads to a theoretical resolution of 70 cm^{-1} , corresponding to a theoretical resolution of 2.8 nm at a wavelength of 633 nm. To reach the OPD maximum, we applied a voltage of 65 V between the combs. To calibrate the mirror position versus the applied voltage, we used a He-Ne laser. The OPD was corrected according to the phase correction described in Ref. 3. To record the interferogram, we moved the mirrors step by step and 100 measurements were acquired at each step (automated procedure). The number of steps was 3000, and the total measurement time was 5 min. The power spectrum retrieved by the Fourier transform of the interferogram is shown in Fig. 5. The spectrum recovered from the lamellar grating interferometer is compared with the spectrum measurement carried out with a monochromator (Jobin Yvon HR 460) that has a spectral resolution of 0.5 nm. One can see that the complex spectral structures of the xenon source coincide. The position accuracy of the emission peaks is better than 0.5 nm. The measured

resolution is 1.6 nm at $\lambda = 400 \text{ nm}$ and 5.5 nm at $\lambda = 800 \text{ nm}$. The wavelength range extends from 380 to 1100 nm. Note that the device was not coated. Therefore almost no spectral contribution was seen beyond 1050 nm. In fact, beyond this wavelength, silicon becomes transparent and therefore only 30% of the incident light (Fresnel reflection) is reflected back by the mirrors. Depending on the required applications, the device can be coated with aluminum or gold.

Conceptually, the only limitation of the lamellar grating interferometer is the ratio a/λ between the grating period and the wavelength. By means of rigorous coupled-wave analysis, it was calculated that, to avoid spectral distortion, this ratio should be greater than 3. Regarding maximum depth d , there is no theoretical limitation. Nevertheless, the lateral mechanical stability of the combs limits the maximum displacement of the mirrors. By means of finite-element simulations of the actuator, we estimated the maximum mechanical displacement at $d = 300 \mu\text{m}$, leading to an OPD δ of $600 \mu\text{m}$. Finally, because of the diffraction, the limited height of the grating ($75 \mu\text{m}$) leads to a maximum practical wavelength. Further investigations will specify these constraints.

A miniature MEMS-based lamellar grating spectrometer has been realized. The dimensions of the MEMS chip are $5 \text{ mm} \times 5 \text{ mm}$. The ability of the device to measure wide wavelength range spectra has been demonstrated. For the first time to our knowledge, from the measured spectrum of a xenon source it has been shown that this device is perfectly suitable for a variety of applications in the visible and the near infrared. Compared with grating-based instruments, this device exploits the advantages of Fourier spectroscopy without the need for a beam splitter. In addition, a single pixel detector is used instead of a CCD line.

O. Manzardo's e-mail address is omar.manzardo@unine.ch.

References

- O. Manzardo, "Micro-sized Fourier spectrometers," Ph.D. dissertation (University of Neuchâtel, Neuchâtel, Switzerland, 2002).
- S. D. Collins, R. L. Smith, C. Gonzàles, K. P. Stewart, J. G. Hagopian, and J. M. Sirota, *Opt. Lett.* **24**, 844 (1999).
- O. Manzardo, H. P. Herzig, C. R. Marxer, and N. F. de Rooij, *Opt. Lett.* **24**, 1705 (1999).
- H. L. Kung, A. Bhatnagar, and D. A. B. Miller, *Opt. Lett.* **26**, 1645 (2001).
- H. L. Kung, S. R. Bhalotra, J. D. Mansell, D. A. B. Miller, and J. S. Harris, *IEEE J. Sel. Top. Quantum Electron.* **8**, 98 (2002).
- J. Strong and G. A. Vanasse, *J. Opt. Soc. Am.* **50**, 113 (1960).
- J. E. Chamberlain, *The Principles of Interferometric Spectroscopy* (Wiley, New York, 1979).
- W. Noell, P.-A. Clerc, L. Dellmann, B. Guldemann, H. P. Herzig, O. Manzardo, C. R. Marxer, K. J. Weible, R. Dändliker, and N. F. de Rooij, *IEEE J. Sel. Top. Quantum Electron.* **8**, 148 (2002).